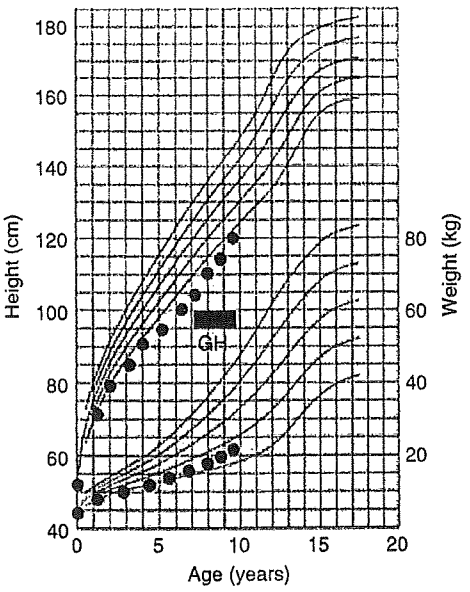

Figure 1 Growth charts of this patient (black circles) plotted on the Japanese sex-matched standard growth curves (+2 S.D., +1 S.D., the mean, −1 S.D., and −2 S.D). The period of GH therapy is indicated.

3 months after consultation with the parents, but the responsiveness to this therapy was not so remarkable (Fig. 1 and Table 2).

Clinical data of the family members are summarized in Table 2. Since endocrine data of the sister and the mother were examined after the investigations of the patient, basal GH values were measured with the Tosoh kit and a Daiichi IRMA kit (Radio Isotope, Tokyo, Japan; endocrine data were not available in the father). In addition, the Daiichi kit was also applied to measure the basal GH in stocked serum samples of the patient, although the serum samples during the provocation tests at 7 years and 1 month of age were not preserved. Notably, the basal GH values of the patient and the sister were obviously different between the two kits, and the GH values in the sister did not show a simple 1:2 ratio between the two kits. The sister and the father had low but normal heights, and the sister had normal endocrine data. The mother had normal clinical findings.

Mutation analysis

This study was approved by the Institutional Review Board Committee at National Center for Child Health and Development. After obtaining written informed consent, leukocyte genomic DNA samples of this patient, the sister, and the parents were amplified by PCR for the coding exons 1–5 and their flanking splice sites of *GH1*, and the PCR products were subjected to direct sequencing on a CEQ 8000 autosequencer (Beckman Coulter, Fullerton, CA, USA). To confirm a heterozygous mutation, the corresponding PCR products were subcloned with a TOPO TA cloning kit (Invitrogen), and wildtype (WT) and mutant (MT) alleles were sequenced separately. The primers used are shown in Table 3, and the primer positions are depicted in Fig. 2A.

Expression analysis

WT-*GH1* from a normal subject and MT-*GH1* from this patient were PCR-amplified with primers GH-1F and GH-5R (Fig. 2A; Table 3) using genomic DNA samples, and the PCR products were subcloned into pCR2.1 plasmid using the TOPO TA cloning kit. Then, *GH1* gene fragments were cleaved from the plasmid DNA with EcoR1 and ligated to the EcoR1 site of an expression vector pRK5. The expression vectors (8 μg) were transiently transfected to SDR-P-1D5 cells obtained from the GH-deficient spontaneous dwarf rat (6),

Table 1 Endocrine studies at 7 years of age.

		Patient		Reference values	
	Stimulus (dosage)	Baseline	Peak	Baseline	Peak
Serum					
GH (ng/ml)[a]	Insulin (0.1 U/kg)	<0.1	<0.1	0.1–20.5	>6.0
	Clonidine (0.1 mg/m^2)	<0.1	<0.1	0.1–20.5	>6.0
	GHRH (1 μg/kg)	<0.1	<0.1	0.1–20.5	>6.0
LH (mIU/ml)	GnRH (100 μg/m^2)	<0.2	5.0	0.0–1.4	0.4–6.0
FSH (mIU/ml)	GnRH (100 μg/m^2)	1.5	19.2	0.6–4.0	6.3–15.6
ACTH (pg/ml)	Insulin (0.1 U/kg)	26.1	179	7.2–22.1	>50
TSH (μU/ml)		1.8		0.44–4.1	
Free T_4 (ng/dl)		1.2		1.03–2.0	
Free T_3 (pg/ml)		3.5		2.40–4.68	
Urine					
GH (pg/mg.cr)[b]		17		>7.0	

Reference values indicate the normal ranges in age-matched Japanese boys (26, 27). Blood sampling during the provocation tests: 0, 15, 30, 60, 90, and 120 mins. IGF-1, insulin-like growth factor-1; T_4, thyroxine; T_3, tri-iodothyronine; and GHRH, growth hormone releasing hormone.
[a]Measured with a Tosoh immunoassay kit.
[b]Measured with a Hitachi immunoassay kit.

Table 2 Summary of clinical data of the family members.

	Patient		Sister	Father	Mother
Age (years)	7 1/12[a]	9 6/12[b]	6 2/12	39	36
Height (cm)	104.5	120.3	105.2	163.0	155.0
Height SDS[c]	−3.0	−2.4	−1.8	−1.5	−0.6
Bone age (years)[d]	3 3/12	5 8/12	NE	NE	NE
GH (ng/ml; Tosoh kit)[e]	<0.1	<0.1[f]	5.23	NE	0.1
GH (ng/ml; Daiichi kit)[e]	1.5	2.86[f]	8.35	NE	0.1
	(0.1–20.5)	(0.1–19.5)	(0.1–21.0)	–	(0.1–3.7)
IGF-1 (ng/ml)	93	140	234	NE	236
	(63–339)	(87–405)	(61–372)	–	(109–265)
IGFBP-3 (ng/ml)	1.36	2.29	2.36	NE	2.79
	(1.76–3.38)	(1.99–3.41)	(1.66–2.91)	–	(1.99–3.19)

IGF-1, insulin-like growth factor-1; IGFBP-3, insulin-like growth factor-binding protein-3; and NE, not examined. The basal hormone values are shown; the values in parentheses represent age- and sex-matched Japanese reference data (26, 27).
[a]Before GH therapy.
[b]On GH therapy.
[c]Assessed by the age- and sex-matched Japanese reference data (28).
[d]Evaluated by the TW-2 method standardized for Japanese (29).
[e]Recombinant GH standard (WHO International Reference Preparation 98/574) has been utilized for the calibration of both kits.
[f]Since blood sample was obtained at 15 h after the GH injection, these values would primarily, if not totally, represent endogenous GH values.

using Gene Pulser Electroporation System (Bio-Rad Laboratories). The transfected cells were incubated for 48 h in a plate with a diameter of 10 cm, and GH in the culture media was measured with the Tosoh and the Daiichi kits. This analysis was performed for three independent experiments. Furthermore, western blotting was performed for the culture media using Rabbit polyclonal GH antibodies (Abs) and anti-Rabbit IgG conjugated with alkaline phosphatase (Promega).

Bioassay

A cell proliferation bioassay was performed for WT-GH and MT-GH, using mouse pro-B cell lymphoma cells that express GH receptor (Ba/F3–hGHR cells) (7). The detailed protocol has been reported previously (8). In brief, WT-GH and MT-GH were prepared in solutions at concentrations of 5, 10, and 20 ng/ml that were determined with the Daiichi kit. Each GH solution of 25 μl was added to 200 μl of Ba/F3–hGHR cell suspension (1×10^5 cells/ml), and the mixture was incubated for 48 h at 37 °C. At the end of the incubation, a colorimetric end point was obtained by an eluted stain bioassay (9), and a bioactive response was determined with a kinetic microplate reader (Molecular Devices, Menlo Park, CA, USA) using optical densities at the test wavelength of 550 nm and a reference wavelength of 650 nm to correct for differential scattering. The experiments were performed in quadruplicate. Statistical significance was examined by Student's *t*-test.

Table 3 Primers utilized in this study.

Primer	Forward Reverse	AT (C) PS (bp)
<Mutation analysis>		
GH-1F	ACAGGTGGGGTCAACAGTGG	60
GH-1R	CCAGGGACCAGGAGCTTTCT	303
GH-2F	CAATCTCAGAAAGCTCCTGG	60
GH-2R	AGCTCCTTAGTCTCCTCCTC	374
GH-3/4F	AGATGAGCACACGCTGAGTG	62
GH-3/4R	AAGGTGAGTTCTCTTGGGTC	584
GH-5F	AGGCCTTTCTCTACACCCTG	60
GH-5R	AGAAGGACACCTAGTCAGAC	435
<Expression analysis>		
GH-1F	ACAGGTGGGGTCAACAGTGG	60
GH-5R	AGAAGGACACCTAGTCAGAC	1727

AT, annealing temperature; and PS, product size.

Protein modeling analysis

The protein conformation was analyzed by Esy-Pred3D (10).

Results

Mutation analysis

Two novel mutations were identified in the patient, a 2 bp deletion at exon 3 (c.280–281delCA) that is predicted to cause a frameshift at the 68th codon for glutamine and resultant termination at the 106th codon (p.Q68fsX106) and a missense mutation at exon 4 (c.426C>G) that is predicted to result in a substitution of aspartic acid with glutamic acid at the 116th codon of GH produced by a novel *GH1* mutation (p.D116E; Fig. 2B). The father and the sister were heterozygous for the p.D116E, and the mother was heterozygous for the p.Q68fsX106 mutation (Fig. 2C).

Functional studies

Expression analysis showed that the p.D116E-GH in the three different culture media was immeasurable with the Tosoh kit but was clearly measurable with the Daiichi kit, and that the p.Q68fsX106-GH was

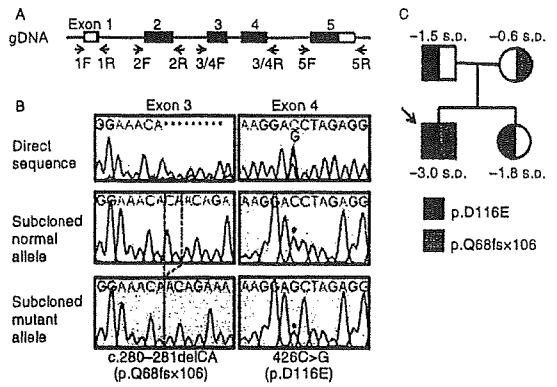

Figure 2 (A) Schematic representation of *GH1*. The black and white boxes on genomic DNA (gDNA) denote the coding regions on exons 1–5 and the UTRs respectively. The arrows indicate the position of the primers utilized in this study. (B) Mutation analysis of *GH1* in this patient. The electrochromatograms delineate the c.280–281delCA (p.Q68fsX106) mutation in exon 3 (left) and the c.426C>G (p.D116E) mutation in exon 4 (right). The mutations have been indicated by the direct sequencing, and confirmed by the subsequently performed sequencing of the subcloned normal and mutant alleles. (C) Pedigree of the family. The height SDS is shown for each family member; for the patient the s.d. before GH therapy is indicated. Of the two mutations identified in this patient, p.D116E is of paternal origin and p.Q68fsX106 is of maternal origin. The sister is heterozygous for the p.D116E mutation.

undetectable by both of the kits (Table 4). Western blot analysis delineated a 22 kDa band for the p.D116E-GH as well as for the WT-GH (Fig. 3A), and a similar band intensity was identified when 3 ng of the p.D116E-GH measured with the Daiichi kit (13 μl of culture media of experiment 3 in Table 4) and 5 ng of WT-GH were utilized. For the p.Q68fsX106-GH, no band was identified for the same amount of culture media (13 μl). Bioassay revealed that the bioactivity was similar between the WT-GH and the p.D116E-GH ($P=0.069$, 0.066, and 0.127 at GH concentrations of 5, 10, and 20 ng/ml based on the Daiichi kit respectively; Fig. 3B). Protein-modeling analysis indicated a normal conformation of the p.D116E-GH (Fig. 3C).

Discussion

This patient had apparently complete GH deficiency and two novel compound *GH1* mutations (p.D116E and p.Q68fsX106). However, his growth pattern including normal birth length, the relatively mild postnatal growth failure, and the poor response to GH therapy is not typical for congenital GH deficiency (11, 12), and the urine GH and serum IGF-1 and IGFBP-3 values indicate a hidden GH activity. Consistent with this, the p.D116E-GH was immeasurable with the Tosoh kit but was measurable with the Daiichi kit, and had an apparently normal *in vitro* biological function. In this regard, the three kits employed in this study utilize two monoclonal

Table 4 GH values in the culture media (ng/ml).

	p.D116E		p.Q68fsX106	
Experiment	Tosoh kit	Daiichi kit	Tosoh kit	Daiichi kit
1	<0.1	90	<0.1	<0.1
2	<0.1	107	<0.1	<0.1
3	<0.1	232	<0.1	<0.1

Abs for GH, one against an epitope within the 22 kDa GH-specific residues (32–46 amino acids) and the other against an epitope specific to each kit. The Hitachi kit detects an epitope at the N-terminal region, while the epitope specifically recognized by the Tosoh and Daiichi kits is unknown. Thus, while the p.Q68fsX106 appears to be an amorphic mutation that is incapable of producing GH probably because of nonsense-mediated mRNA decay (13), it is likely that the p.D116E affects the GH epitope primarily recognized by the Tosoh kit but not by the Hitachi or the Daiichi kit, thereby producing a possible immunologically anomalous but biologically active GH. This notion would also explain why the basal serum GH values measured with the Tosoh kit were obviously lower than those measured with the Daiichi kit in the patient and the sister with p.D116E.

It remains to be determined, however, whether the p.D116E-GH has a normal biological function *in vivo*. Although the *in vitro* bioassay indicated an apparently normal function for the p.D116E-GH, it is known that

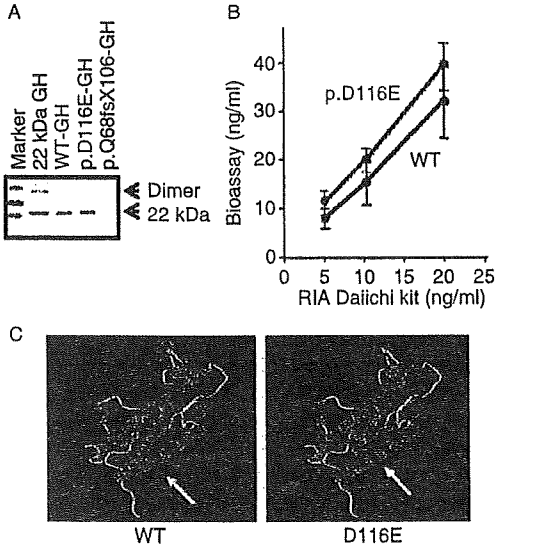

Figure 3 (A) Western blot analysis, showing the presence of 22 kDa WT-GH and p.D116E-GH. The standard 22 kDa human GH is used as an internal control (8). Note that a similar band intensity is delineated for 3 ng of the p.D116E-GH and 5 ng of WT-GH measured with the Daiichi kit. (B) Bioassay of the WT-GH and the p.D116E-GH, using Ba/F3–hGH receptor cells. The results are expressed using the mean and the s.d. (C) Ribbon diagrams of the GH proteins. The white arrows indicate the 116 residue for WT-GH and the p.D116E-GH.

the results obtained with artificially constructed cell lines do not necessarily reflect the *in vivo* biological effects of hGH MTs (8, 14). Indeed, the difference in the GH value between the two kits in the sister and the relationship between the GH value and the band intensity in the western blotting may imply that the p.D116E-GH was not measured precisely even with the Daiichi kit, so that a relatively large amount of the p.D116E-GH was probably utilized in the *in vitro* bioassay, compensating for a possible hypofunction of the p.D116E-GH. Furthermore, since the previously described p.D116A-GH harboring a missense mutation within the GH receptor-binding site 2 has a 5.7-fold lower affinity to the GH receptor than the WT-GH (15), this would argue for a functional importance of the D116 residue and implicate a similar functional alteration of the p.D116E-GH. In addition, although *GH1* missense mutations reported to date are relatively rare (16), GH missense MTs, including those within or near the GH receptor binding site 2, frequently have a reduced or altered biological activity (2, 4, 17–21).

In this regard, comparison of clinical data between the patient with functional hemizygosity for the p.D116E and the mother with functional hemizygosity for the WT *GH1* would suggest that the p.D116E-GH has a reduced, though not abolished, *in vivo* bioactivity (Table 2). In support of this, most individuals with heterozygous *GH1* deletions have normal stature (22) as observed in the mother, while this patient had short stature. It may also be possible that the p.D116E-GH is less secreted from the pituitary into the circulation when compared with an intact GH protein, although the clinical findings of the father and the sister heterozygous for the p.D116E would argue against the possibility that the p.D116E-GH exerts an obvious dominant negative effect (Table 2). However, since short stature is a highly heterogeneous phenotype subject to multiple genetic and environmental factors (23, 24), some factors other than the *GH1* mutations may be involved in the development of short stature in this patient. In addition, there may be an ascertainment bias, because GH-related studies are almost exclusively performed in individuals with short stature. Further studies will permit to clarify the *in vivo* biological function of the p.D116E-GH and its relevance to the development of short stature.

Such an immunologically anomalous and biologically active hormone has been reported previously. It is known that the common LH variant (V-LH) with two completely linked Trp8Arg and Ile15Thr substitutions in the LHβ-subunit is immunologically undetectable when a MAB recognizing an epitope present in the intact LH α/β dimer is utilized, but is measurable when two monoclonal Abs recognizing specific sites in the LHβ subunit are utilized (25). Notably, the V-LH appears to have somewhat weaker bioactivity than the WT-LH, and is often associated with the primary ovarian dysfunction in the Japanese population (25). Nevertheless, elevated LH values characteristic of primary ovarian dysfunction cannot be identified without applying the method using two monoclonal Abs, although FSH values are definitely increased. Thus, when a discrepancy is present between values of a specific hormone and other biochemical data or clinical findings, it is recommended to measure the specific hormone with a different kit, to avoid the misdiagnosis of hormone deficiency.

In summary, we identified an immunologically anomalous but considerably bioactive GH produced by p.D116E mutation. Indeed, such abnormalities along the GH/IGF-1 axis may also be identified by performing GH-related endocrine studies in children with short stature. The presence of such an apparently immeasurable but bioactive hormone, as well as a measurable but bioinactive hormone, should be kept in mind, to allow for an appropriate assessment of endocrine data.

Declaration of interest

The authors declare no conflict of interest.

Funding

This research was supported by Grants for Child Health and Development and Research on Children and Families from the Ministry of Health, Labor, and Welfare.

References

1 Growth Hormone Research Society. Consensus guidelines for the diagnosis and treatment of growth hormone (GH) deficiency in childhood and adolescence: summary statement of the GH Research Society. *Journal of Clinical Endocrinology and Metabolism* 2000 **85** 3990–3993.

2 Takahashi Y, Shirono H, Arisaka O, Takahashi K, Yagi T, Koga J, Kaji H, Okimura Y, Abe H, Tanaka T & Chihara K. Biologically inactive growth hormone caused by an amino acid substitution. *Journal of Clinical Investigations* 1997 **100** 1159–1165.

3 Besson A, Salemi S, Deladoëy J, Vuissoz JM, Eblé A, Bidlingmaier M, Bürgi S, Honegger U, Flück C & Mullis PE. Short stature caused by a biologically inactive mutant growth hormone (GH-C53S). *Journal of Clinical Endocrinology and Metabolism* 2005 **90** 2493–2499.

4 Millar DS, Lewis MD, Horan M, Newsway V, Easter TE, Gregory JW, Fryklund L, Norin M, Crowne EC, Davies SJ, Edwards P, Kirk J, Waldron K, Smith PJ, Phillips JA III, Scanlon MF, Krawczak M, Cooper DN & Procter AM. Novel mutations of the growth hormone 1 (GH1) gene disclosed by modulation of the clinical selection criteria for individuals with short stature. *Human Mutation* 2003 **21** 424–440.

5 Tanae A, Maesaka I, Tanaka T, Yokoya S & Tachibana K. *Therapy for Pediatric Endocrinological Disease*, pp. 1–3, Tokyo: Shindan to Chiryou, 2007 (in Japanese).

6 Nogami H, Takeuchi T, Suzuki K, Okuma S & Ishikawa H. Studies on prolactin and growth hormone gene expression in the pituitary gland of spontaneous dwarf rats. *Endocrinology* 1989 **125** 964–970.

7 Wada M, Uchida H, Ikeda M, Tsunekawa B, Naito N, Banba S, Tanaka E, Hashimoto Y & Honjo M. The 20 kDa human growth hormone (hGH) differs from the 22 kDa hGH in the complex

formation with cell surface hGH receptor and hGH-binding protein circulating in human plasma. *Molecular Endocrinolgy* 1998 **12** 146–156.
8 Ishikawa M, Nimura A, Horikawa R, Katsumata N, Arisaka O, Wada M, Honjo M & Tanaka T. A novel specific bioassay for serum human growth hormone. *Journal of Clinical Endocrinology and Metabolism* 2000 **85** 4274–4279.
9 Baley PA, Yateman ME, Sandhu R, Dattani MT, Hassan MK, Holt SJ & Marshall NJ. The development of an eluted stain bioassay (ESTA) for human growth hormone. *Growth Regulation* 1995 **5** 36–44.
10 Lambert C, Léonard N, De Bolle X & Depiereux E. ESyPred3D: prediction of proteins 3D structures. *Bioinformatics* 2002 **18** 1250–1256.
11 Laron Z & Silbergeld A. A simple diagnostic screening test for children with short stature – with emphasis on genetic defects along the GH axis. *Pediatric Endocrinology Reviews* 2007 **4** 96–98.
12 Tanaka T, Cohen P, Clayton PE, Laron Z, Hintz RL & Sizonenko PC. Diagnosis and management of growth hormone deficiency in childhood and adolescence – part 2: growth hormone treatment in growth hormone deficient children. *Growth Hormone and IGF Research* 2002 **12** 323–341.
13 Holbrook JA, Neu-Yilik G, Hentze MW & Kulozik AE. Nonsense-mediated decay approaches the clinic. *Nature Genetics* 2004 **36** 801–808.
14 Popii V & Baumann G. Laboratory measurement of growth hormone. *Clinica Chimica Acta* 2004 **350** 1–16.
15 Cunningham BC, Ultsch M, De Vos AM, Mulkerrin MG, Clauser KR & Wells JA. Dimerization of the extracellular domain of the human growth hormone receptor by a single hormone molecule. *Science* 1991 **254** 821–825.
16 Wagner JK, Eblé A, Hindmarsh PC & Mullis PE. Prevalence of human GH-1 gene alterations in patients with isolated growth hormone deficiency. *Pediatric Research* 1998 **43** 105–110.
17 Lewis MD, Horan M, Millar DS, Newsway V, Easter TE, Fryklund L, Gregory JW, Norin M, Del Valle CJ, López-Siguero JP, Cañete R, López-Canti LF, Díaz-Torrado N, Espino R, Ulied A, Scanlon MF, Procter AM & Cooper DN. A novel dysfunctional growth hormone variant (Ile179Met) exhibits a decreased ability to activate the extracellular signal-regulated kinase pathway. *Journal of Clinical Endocrinology and Metabolism* 2004 **89** 1068–1075.
18 Binder G, Keller E, Mix M, Massa GG, Stokvis-Brantsma WH, Wit JM & Ranke MB. Isolated GH deficiency with dominant inheritance: new mutations, new insights. *Journal of Clinical Endocrinology and Metabolism* 2001 **86** 3877–3881.
19 Deladoëy J, Stocker P & Mullis PE. Autosomal dominant GH deficiency due to an Arg183His GH-1 gene mutation: clinical and molecular evidence of impaired regulated GH secretion. *Journal of Clinical Endocrinology and Metabolism* 2001 **86** 3941–3947.
20 Salemi S, Yousefi S, Baltensperger K, Robinson IC, Eblé A, Simon D, Czernichow P, Binder G, Sonnet E & Mullis PE. Variability of isolated autosomal dominant GH deficiency (IGHD II): impact of the P89L GH mutation on clinical follow-up and GH secretion. *European Journal of Endocrinology* 2005 **153** 791–802.
21 Dattani MT, Hindmarsh PC, Brook CG, Robinson IC, Kopchick JJ & Marshall NJ. G120R, a human growth hormone antagonist, shows zinc-dependent agonist and antagonist activity on Nb2 cells. *Journal of Biological Chemistry* 1995 **270** 9222–9226.
22 Phillips JA III & Cogan JD. Genetic basis of endocrine disease. 6. Molecular basis of familial human growth hormone deficiency. *Journal of Clinical Endocrinology and Metabolism* 1994 **78** 11–16.
23 Visscher PM. Sizing up human height variation. *Nature Genetics* 2008 **40** 489–490.
24 Vogel F & Motulsky AG. *Human Genetics: Problems and Approaches* Berlin/Heidelberg/New York/Tokyo: Springer-Verlag, 1986.
25 Themmen APN & Huhtaniemi IT. Mutations of gonadotropins and gonadotropin receptors: elucidating the physiology and pathophysiology of pituitary–gonadal function. *Endocrine Reviews* 2000 **21** 551–583.
26 Japan Public Health Association. *Normal Biochemical Values in Japanese Children* Tokyo: Sanko Press, 1996 (in Japanese).
27 Inada H, Imamura T & Nakajima R. *Manual of Endocrine Examination for Children*, pp. 14–22, Osaka: Medical Review, 2002 (in Japanese).
28 Suwa S, Tachibana K, Maesaka H, Tanaka T & Yokoya S. Longitudinal standards for height and height velocity for Japanese children from birth to maturity. *Clinical Pediatric Endocrinology* 1992 **1** 5–13.
29 Murata M, Matsuo N, Tanaka T, Ohtsuki F, Ashizawa K, Tatara H, Anzo M, Sato M, Matsuoka H, Asami T & Tsukakoshi K. *Radiographic Atlas of Skeletal Development for the Japanese* Tokyo: Kanehara Press, 1993 (in Japanese).

Received 19 May 2009
Accepted 19 May 2009

Mini Review

HORMONE RESEARCH

Horm Res 2009;71:245–252
DOI: 10.1159/000208797

Received: July 25, 2008
Accepted: January 12, 2009
Published online: April 1, 2009

MAMLD1 (CXorf6): A New Gene Involved in Hypospadias

Tsutomu Ogata[a] Jocelyn Laporte[b] Maki Fukami[a]

[a]Department of Endocrinology and Metabolism, National Research Institute for Child Health and Development, Tokyo, Japan, and [b]Department of Molecular Pathology, Institut de Génétique et de Biologie Moléculaire et Cellulaire, Centre Universitaire de Strasbourg, Illkirch, France

Key Words
MAMLD1 · *CXorf6* · Hypospadias · Testosterone

Abstract
MAMLD1 (mastermind-like domain containing 1), previously known as *CXorf6* (chromosome X open reading frame 6), has been shown to be a causative gene for hypospadias. This is primarily based on the identification of nonsense mutations (E124X, Q197X, and R653X), which undergo nonsense-mediated mRNA decay, in patients with penoscrotal hypospadias. Subsequent studies have shown that (1) the mouse homolog is transiently expressed in fetal Sertoli and Leydig cells around the critical period of sex development; (2) transient knockdown of *Mamld1* results in significantly reduced testosterone production in murine Leydig tumor cells; (3) MAMLD1 protein shares homology to mastermind-like 2 (MAML2) protein that functions as a co-activator in canonical Notch signaling; (4) MAMLD1 localizes to the nuclear bodies and transactivates the promoter activity of a non-canonical Notch target gene hairy/enhancer of split 3 *(Hes3)*, rather than the canonical Notch target genes such as *Hes1* and *Hes5*, without demonstrable DNA-binding capacity, and (5) *MAMLD1* is regulated by steroidogenic factor 1. These findings suggest that the *MAMLD1* mutations cause hypospadias primarily because of compromised testosterone production around the critical period of sex development, and provide useful information for the molecular network involved in fetal testosterone production.

Introduction

Hypospadias is defined by the urethral opening on the ventral side of the penis, and is classified into mild glandular or penile type and severe penoscrotal or perineal type [1]. It is a mild form of 46,XY disorders of sex development (DSD), and affects ~0.5% of male newborns [2]. Hypospadias is primarily caused by compromised androgen effects, and appears as an isolated anomaly or in association with other genital anomalies such as micropenis and cryptorchidism. To date, while mutation analyses have been performed for multiple genes involved in androgen effects such as *SRD5A2* for 5α-redeuctase and *AR* for androgen receptor, pathologic mutations have been identified only in a very small portion of patients [2]. This would be consistent with hypospadias being a highly heterogeneous condition subject to multiple genetic and environmental factors. Indeed, several candidate genes such as *ATF3*, *FKBP52*, *FGFR2*, *FGF8*, *FGF10*, and *BMP7* have been identified, and multiple susceptibility factors for hypospadias have been found in several genes such as *ESR1*, *ESR2*, and *SRD5A2* [3–7].

We have recently shown that *CXorf6* (chromosome X open reading frame 6) is a novel gene for hypospadias [8], and coined a new gene symbol *MAMLD1* (mastermind-like domain containing 1) on the basis of its characteristic protein structure [9]. Here, we review the current knowledge about *MAMLD1*.

KARGER

Fax +41 61 306 12 34
E-Mail karger@karger.ch
www.karger.com

0301–0163/09/0715–0245$26.00/0

Accessible online at:
www.karger.com/hre

Dr. Tsutomu Ogata
Department of Endocrinology and Metabolism
National Research Institute for Child Health and Development
2-10-1 Ohkura, Setagaya, Tokyo 157-8535 (Japan)
Tel. +81 3 5494 7025, Fax +81 3 5494 7026, E-Mail tomogata@nch.go.jp

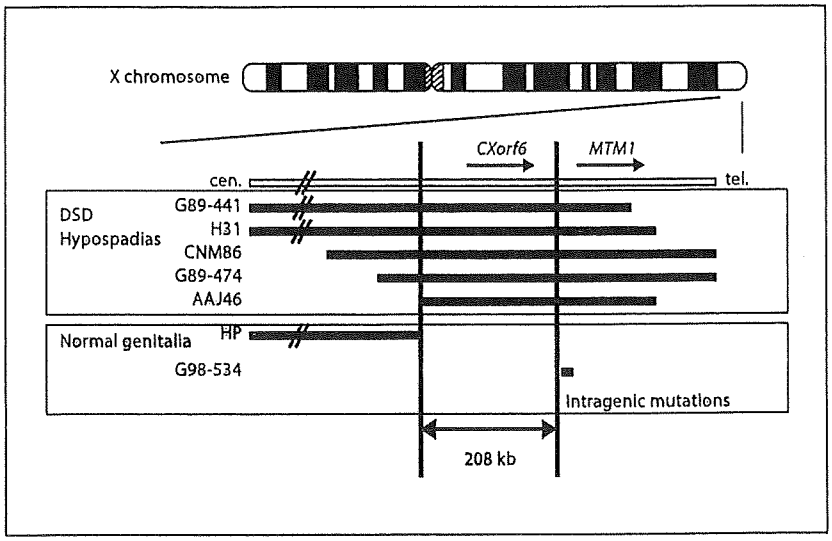

Fig. 1. Identification of *CXorf6* as a candidate DSD gene on Xq28 by deletion mapping. The horizontal bars indicate the deleted segments in each case. Of the 7 male patients with microdeletions around *MTM1* for myotubular myopathy, 5 show 46,XY DSD (primarily hypospadias), whereas 2 patients have normal genitalia as do patients with intragenic *MTM1* mutations. The smallest overlapping deleted region is roughly 208 kb in physical length, and contains *CXorf6* as a sole gene within the critical region.

Cloning of a Candidate Gene for 46,XY DSD

A gene for 46,XY DSD has been postulated around *MTM1* for myotubular myopathy on Xq28, on the basis of the finding that genital development is normal in patients with intragenic *MTM1* mutations, and invariably abnormal in 6 patients with microdeletions involving *MTM1* [10–13]. The 6 patients consist of 3 sporadic and 3 familial cases, and 5 of them have glandular, penile, or penoscrotal hypospadias and the remaining 1 patient exhibits ambiguous genitalia [10–12]. These findings suggest that a gene for 46,XY DSD, especially that for hypospadias, resides in the vicinity of *MTM1*, and that loss or disruption of the gene results in the development of 46,XY DSD as consequence of a contiguous gene deletion syndrome.

In 1997, Laporte et al. [14] identified *MAMLD1* (named *CXorf6* at that time) from a 430-kb region deleted in 2 sporadic cases with myotubular myopathy and 46,XY DSD [12]. *MAMLD1* comprises at least 7 exons, and harbors an open reading frame on exons 3–6 that is predicted to produce 2 proteins of 701 and 660 amino acids as a result of in-frame alternative splicing with and without exon 4. Furthermore, subsequent studies have shown loss of *MAMLD1* in all patients with myotubular myopathy and 46,XY DSD (fig. 1), and no other candidate gene for 46,XY DSD has been identified within the commonly deleted region. These findings imply that *MAMLD1* is an excellent candidate gene for 46,XY DSD, especially hypospadias.

MAMLD1 Mutations in Hypospadiac Patients

We performed direct sequencing for the coding exons 3–6 and their flanking splice sites of *MAMLD1* in 166 patients with various types of DSD or abnormal external genitalia. They consisted of 117 Japanese patients (113 sporadic cases and 4 probands of familial cases), 45 European patients (39 sporadic cases and 6 probands of familial cases), and 4 Chinese patients (4 probands of familial cases). The 117 Japanese patients comprised: 19 cases with gonadal dysgenesis (10 with complete type and 9 with incomplete type) with no demonstrable mutation in the known or candidate sex development genes *SRY*, *DMRT1*, *SF1*, and *LHX9* [2]; 2 cases with 46,XY DSD of unknown cause; 56 cases with hypospadias (16 with glandular type, 16 with penile type, 20 with penoscrotal type, and 4 with perineal type), and 40 cases with isolated cryptorchidism (33 with unilateral inguinal or abdominal type and 7 with bilateral inguinal type). All the Japanese patients had a normal male karyotype and lacked extragenital features except for short stature in 6 cases, mental retardation in 3 cases, and multiple congenital anomalies in 2 cases. Thus, most patients exhibited abnormal external genitalia as the sole recognizable abnormality. The 49 European and Chinese patients had various types of abnormal genitalia, ranging from hypospadias to feminized genitalia (detailed phenotypes are unknown).

Consequently, 3 nonsense mutations were identified in Japanese patients with hypospadias: E124X in mater-

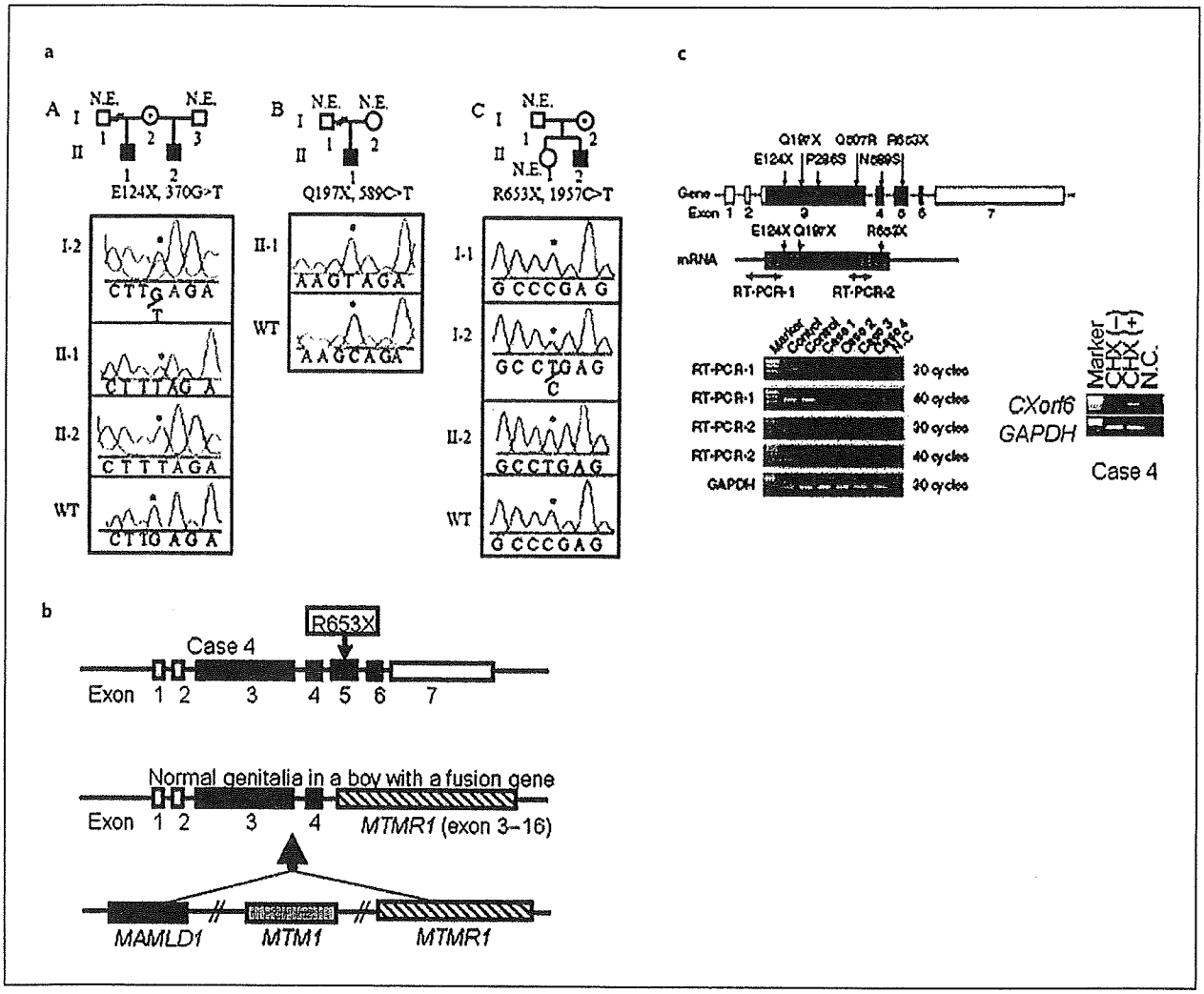

Fig. 2. Molecular findings in patients with nonsense mutations. **a**, **b** adapted from Fukami et al. [8, 9]. **a** The pedigrees and electrochromatograms of Japanese patients with nonsense mutations (A–C). The black squares indicate the patients with 46,XY DSD and the mutant *MAMLD1*, and the circles with dots represent molecularly confirmed carrier females. The asterisks in the chromatograms indicate the mutant and the corresponding wild-type nucleotides. NE = Not examined. **b** Schematic representation of the R653X mutation in case 4 and the fusion gene between *MAMLD1* and *MTMR1*. The black and the white squares in *MAMLD1* indicate the translated and untranslated regions, respectively. **c** The NMD analysis. The black and gray boxes represent the coding regions, and the open boxes denote the untranslated regions. The positions of the mutations and variations are shown. RT-PCR for the two regions (RT-PCR-1 and 2) has produced no bands after 30 cycles and very faint bands after 40 cycles in cases 1–4. In case 4, no band is seen without an NMD inhibitor cycloheximide (CHX), whereas a clear band is delineated with CHX treatment.

nally related half brothers from family A (cases 1 and 2); Q197X in a patient from family B (case 3), and R653X in a patient from family C (case 4; fig. 2a) [3]. The mothers of families A and C were heterozygous for the mutations, although the mother of family B was not studied. In addition to the 3 nonsense mutations, we also found 3 apparently non-pathologic variants: P286S and Q507R that were not co-segregated with the 46,XY DSD in affected families, and a previously reported polymorphism N589S *(rs2073043)* [3].

Table 1. Clinical findings of the 4 Japanese cases with *MAMLD1* nonsense mutations

	Case 1	Case 2	Case 3	Case 4
Genital findings				
Gestational age, weeks	39	40	40	41
Birth length, cm	51.0 (+1.0 SD)	49.5 (+0.2 SD)	50.5 (+0.7 SD)	47.5 (–0.7 SD)
Birth weight, kg	3.61 (+1.5 SD)	3.40 (+1.0 SD)	3.21 (+0.5 SD)	2.94 (–0.2 SD)
Age at exam	4 months	1 month	2 years	1 month
Clinical diagnosis	Hypospadias with chordee	Hypospadias with chordee	Hypospadias with chordee	Hypospadias with chordee
Urethral meatus	Penoscrotal junction	Penoscrotal junction	Penoscrotal junction	Penoscrotal junction
Age at urethroplasty, years	2.5	3.9	6.0 and 6.6	1.9
Penile length, cm	2.5 (–1.5 SD)	2.5 (–1.5 SD)	2.0 (–3.4 SD)	1.2 (–3.5 SD)
Testis size, ml	1–2 (B) (WNR)	1–2 (B) (WNR)	1 (B) (WNR)	1–2 (B) (WNR)
Testis position	Inguinal (B)	Scrotal	Scrotal	Retractile (B)
Age at orchidopexy, years	6.3	–	–	1.9
Scrotal appearance	Bifid and hypoplastic	Bifid	Bifid	Bifid
Wolffian structures	Normal on MRI	Normal on MRI	NE	NE
Müllerian structures	Absent on MRI	Absent on MRI	NE	NE
Renal structures	Normal on MRI	Normal on MRI	Normal on ultrasounds	NE
Serum hormone values				
Age at exam	4 months	1 month	2 years	3 months
LH, IU/l	1.2 (0.1–4.7)	3.1 (0.1–4.7)	0.2 (<0.2–3.1)	NE
FSH, IU/l	1.5 (0.4–5.7)	2.2 (0.4–5.7)	1.6 (0.2–5.2)	NE
Testosterone, nmol/l	1.4 (0.1–12.0)→9.0 (7.0–15.0)[a]	9.0 (4.0–14.0)	0.1 (0.1–1.0)	9.4 (4.0–14.0)
DHT, nmol/l	0.8 (0.2–4.5)→3.7 [a]	1.2 (0.2–4.5)	NE	NE
Age at exam, years:months	2:05	2:05	4:00	6:03
LH, IU/l	0.2 (<0.2–3.1)→3.5 (1.4–6.0)[b]	0.2 (<0.2–3.1)	<0.2 (<0.2–1.2)	0.2 (<0.2–1.4)
FSH, IU/l	<0.2 (0.2–5.2)→1.5 (2.3–6.9)[b]	0.8 (0.2–5.2)	1.6 (0.7–3.0)	1.2 (0.3–4.0)
Testosterone, nmol/l	<0.3 (0.1–1.0)→10.1 (7.0–15.0)[a]	0.7 (0.1–1.0)	<0.3 (<0.5)	0.3 (<0.5)
DHT, nmol/l	0.07 (0.05–2.0)→2.84[a]	<0.15 (0.05–2.0)	NE	NE

SD = Standard deviation; NE = not examined; B = bilateral; MRI = magnetic resonance imaging; WNR = within the normal range (1–2 ml before puberty); ND = not determined; LH = luteinizing hormone; FSH = follicle-stimulating hormone; DHT = dihydrotestosterone.

Assessments of body sizes (length, height, weight, and head circumference), penile length, testis size, and menarchial age are based on the Japanese reference data. The hormone values in parentheses represent the age- and sex-matched normal range in the Japanese; the reference data for serum hormones are based on the literature.

[a] After a human chorionic gonadotropin stimulation (3,000 IU/m^2/dose i.m. for 3 consecutive days; blood sampling on day 4).

[b] Peak values during a gonadotropin-releasing hormone test (100 μg/m^2 bolus i.v.; blood sampling at 0, 30, 60, 90, and 120 min).

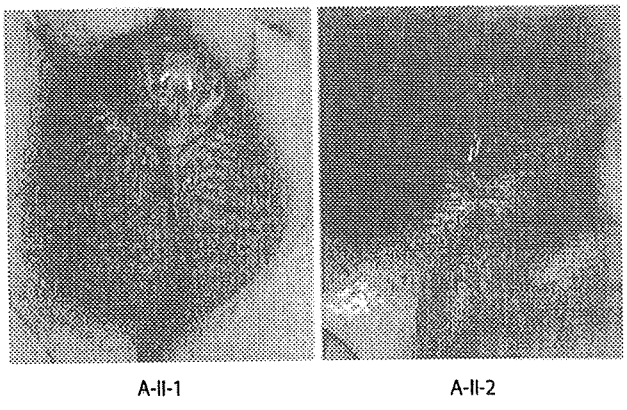

Fig. 3. External genital findings of cases 1 and 2.

Nonsense-Mediated mRNA Decay

When the 3 nonsense mutations were identified, one problem was that hypospadias in case 4 with R653X on exon 5 may be inconsistent with apparently normal genital development in a previously reported boy with a microdeletion involving *MTM1* that resulted in the generation of a fusion gene between exons 1–4 of *MAMLD1* and exons 3–16 of *MTMR1* (locus order: *MAMLD1–MTM1–MTMR1*), because the coding exons 3 and 4 are preserved in both case 4 and the boy with the fusion gene [15] (fig. 2b). However, in contrast to the positive expression of the fusion gene [15], the 3 nonsense mutations are predicted to cause nonsense-mediated mRNA decay (NMD) because of their positions [16]. Consistent with this, RT-

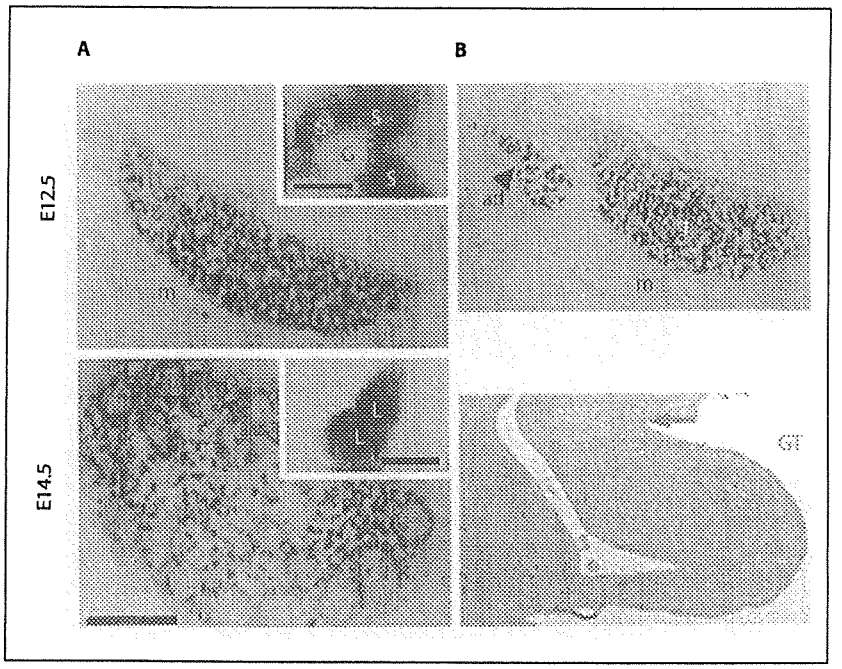

Fig. 4. In situ hybridization analysis of the murine *Mamld1*. **a** Expression patterns in the fetal testes at E12.5 and E14.5. The blue signals are derived from in situ hybridization for *Mamld1*, and the brown signals from immunohistochemical staining with Sf-1 (Ad4bp) antibodies. m = Mesonephros; G = germ cell; S = Sertoli cell; L = Leydig cell. The scale bars in the low and high power fields represent 200 and 20 μm, respectively. Adapted from Fukami et al. [8]. **b** Expression patterns in the fetal adrenal (upper part) and external genitalia (lower part) of male mouse at E12.5. m = Mesonephros; g = gonad; ad = adrenal; GT = genital tubercle (the region between two arrows). *MAMLD1* is not expressed in the adrenal, and weakly and diffusely expressed in the external genitalia as in other non-genital skin tissues.

PCR from leukocytes indicated drastically reduced transcripts in cases 1–4 (fig. 2c) [3, 4]. Furthermore, the NMD was prevented by the NMD inhibitor cycloheximide, providing further support for the occurrence of NMD in the 3 nonsense mutations. The occurrence of NMD was also demonstrated in the carrier mothers [4]. Thus, although the NMD has not been confirmed in the testicular tissue, the results explain the apparent discordance in the genital development between case 4 and the boy described by Tsai et al. [15], and indicate that the 3 nonsense mutations including R653X are pathologic mutations.

Phenotypes in Mutation-Positive Patients

Cases 1–4 had penoscrotal hypospadias with chordee as the conspicuous genital phenotype, in association with other genital phenotypes (fig. 3, table 1). Pituitary-gonadal serum hormone values remained within the normal range, including the human chorionic gonadotropin (hCG)-stimulated testosterone value in case 1 at 2 years and 5 months of age, and the basal testosterone values in case 2 at 1 month of age and in case 4 at 3 months of age when serum testosterone is physiologically elevated. Thus, the diagnosis of idiopathic hypospadias was initially made in cases 1–4.

In situ Hybridization Analysis for Mouse *Mamld1*

In situ hybridization analysis for mouse *Mamld1* showed a cell type-specific expression pattern [3]. Namely, *Mamld1* is specifically and transiently expressed in Sertoli and Leydig cells around the critical period of sex development (E12.5–E14.5; fig. 4a). This expression pattern has been confirmed by double staining with antibodies for Ad4bp/Sf-1 that serves as a marker for Sertoli and Leydig cells [17–19]. In extragonadal tissues at E12.5, *Mamld1* expression was absent in the adrenals and weakly and diffusely identified in the external genital region including the genital tubercle at a level similar to that detected in the neighboring extragenital tissues (fig. 4b). *Mamld1* was also clearly expressed in the müllerian ducts, forebrain, somite, neural tube, and pancreas. By contrast, *Mamld1* expression was absent in the postnatal testes. These data imply that nonsense mutations of *MAMLD1* cause hypospadias primarily because of transient testicular dysfunction and resultant compromised testosterone production around the critical period of sex development, and explain why postnatal endocrine data were normal in cases 1–4.

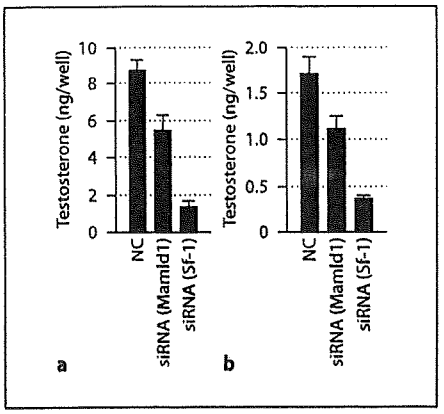

Fig. 5. Effects of siRNA on testosterone production in the mouse Leydig tumor (MLT) cells. Adapted from Fukami et al. [9]. Relative mouse *CXorf6* and *Sf-1* mRNA levels have been reduced to 25–30% in the MLT cells after 48 h of incubation with two siRNAs. NC = Negative control transfected with non-targeting RNA. **a** Testosterone concentration in the medium after 48 h of incubation with siRNAs. **b** Testosterone concentration in the medium after 1 h of incubation with hCG using the MLT cells cultured with siRNA for 48 h.

Function of *Mamld1* in Testosterone Production

We performed knockdown analysis with siRNAs for *Mamld1* using mouse Leydig tumor cells that retain the capability of testosterone production and the responsiveness to hCG stimulation [4]. When the mRNA level of endogenous *Mamld1* was severely reduced in the mouse Leydig tumor cells (25–30%), testosterone production was decreased to 50–60% after 48 h of incubation and 1 h after hCG stimulation (fig. 5). However, the testosterone reduction was much milder than that caused by siRNAs for *Sf-1* (fig. 5; our unpublished observation). The results were confirmed with 2 different siRNAs. This implies that *MAMLD1* is involved in testosterone biosynthesis. Furthermore, since testosterone production would probably be attenuated rather than abolished in the absence of *MAMLD1*, this is consistent with the hypospadias phenotype in the affected patients [2].

Sf-1 Controls *Mamld1*

Mouse *Mamld1* is co-expressed with *Ad4bp/Sf-1*, and *SF-1* is known to regulate the transcription of a vast array of genes involved in sex development by binding to specific DNA sequences [17–19]. This implies that *Mamld1* is also controlled by *Sf-1*. Consistent with this notion, human *MAMLD1* harbors a putative SF-1-binding sequence 'CCAAGGTCA' at intron 2 upstream of the coding region [4]. This binding site also resides at intron 1 upstream of the coding region of the mouse *Mamld1*. Furthermore, we performed DNA binding and luciferase assays, showing that SF-1 protein binds to the putative target sequence and exerts a transactivation function [4]. These findings argue for the possibility that Mamld1 expression is regulated by *Sf-1*.

Functional Studies of MAMLD1 Protein

We found that MAMLD1 protein has a unique structure with homology to that of mastermind like 2 (MAML2) protein (fig. 6a) [4]. A unique amino acid sequence, which we designate mastermind-like (MAML) motif, was inferred from sequence alignment with MAML1, MAML2, and MAML3 proteins. The MAML motif was well conserved among MAMLD1 orthologs identified in frogs, birds, and mammals. In addition, glutamine-rich, proline-rich, and serine-rich domains were identified in MAMLD1.

MAML2 is a non-DNA-binding transcriptional coactivator in Notch signaling that plays an important role in cell differentiation in multiple tissues by exerting either inductive or inhibiting effects according to the context of the cells [20–22]. Upon ligand-receptor interaction, the Notch intracellular domain (N-ICD) is translocated from the cell surface to the nucleus and interacts with a DNA-binding transcription factor, recombination signal binding protein-J (RBP-J), to activate target genes like hairy/enhancer of split 1 *(Hes1)* and *Hes5* [23]. In this canonical Notch signaling process, MAML2 forms a ternary complex with N-ICD and RBP-J at nuclear bodies, enhancing the transcription of the Notch target genes [20, 21, 24–26]. In addition to such canonical Notch target genes, recent studies have shown that *Hes3* can be induced by stimulation with a Notch ligand, via a STAT3 (signal transducer and activator of transcription 3)-mediated pathway [27]. This finding, together with lack of *Hes3* induction by N-ICD [22], implies that *Hes3* represents a target gene of a non-canonical Notch signaling.

Thus, we first examined whether MAMLD1 localizes to the nuclear bodies, as observed for MAML2 [4]. Since PCR-based human cDNA library screening has revealed that the exon 4-positive splice variant is more strongly expressed than the exon 4-negative splice variant (ΔExon 4) [3], functional studies were performed primarily with

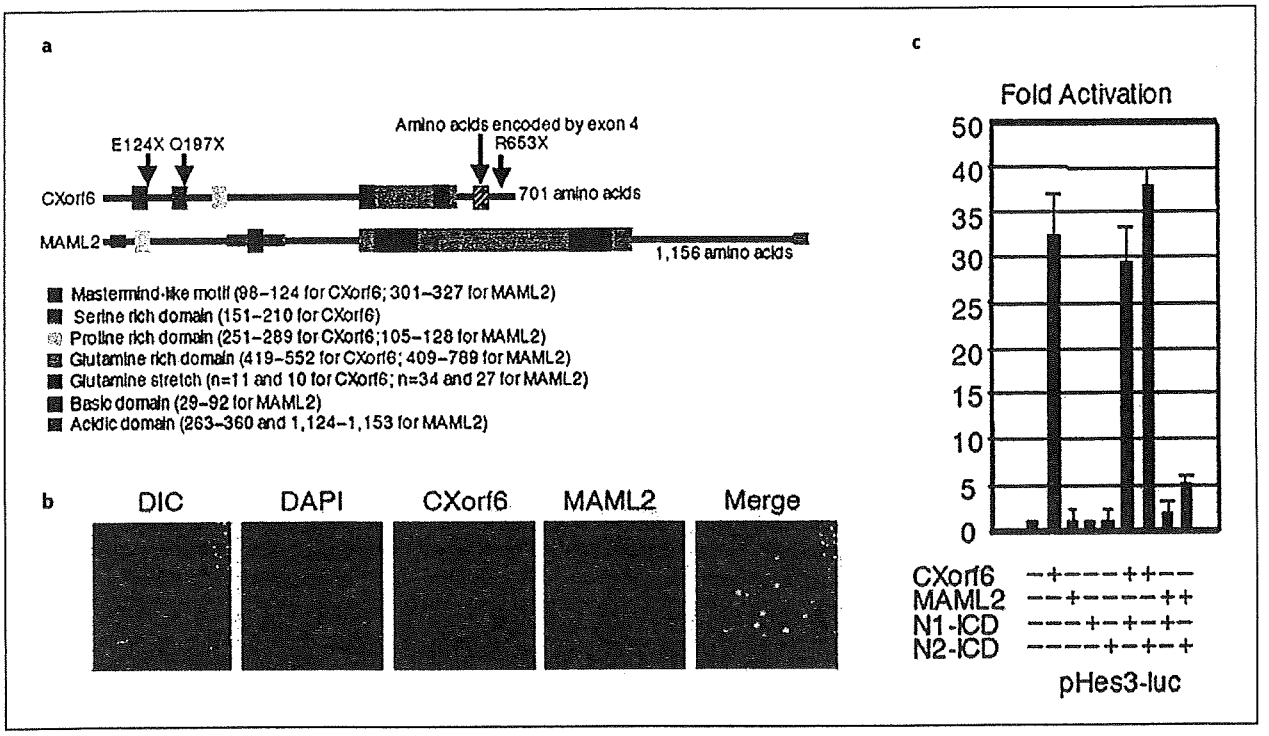

Fig. 6. Functional studies of the wild-type MAMLD1 protein. Adapted from Fukami et al. [9]. **a** Protein structure analysis. The structure of human CXorf6 (MAMLD1) and MAML2 proteins. The identified domains are shown, together with the positions of the three nonsense mutations. **b** Subcellular localization analysis, showing co-localization of the wild-type MAMLD1 and MAML2 in the nuclear bodies. **c** Transactivation functions for the promoter of *Hes3*. + = Presence of expression vectors with cDNAs for *MAMLD1, MAML2, N1-ICD* (Notch 1 intracellular domain), and *N2-ICD* (Notch 2 intracellular domain); − = presence of expression vector only (empty).

the exon 4-positive splice variant (thereafter, this variant is simply described as *MAMLD1*). MAMLD1 was distributed in a speckled pattern and co-localized with the MAML2 protein (fig. 6b). Furthermore, while the E124X and Q197X fusion proteins resided in the nucleus, they were incapable of localizing to the nuclear bodies. The R653X and apparently non-pathologic missense proteins showed a punctate pattern, and co-localized with the wild-type MAMLD1.

Next, we studied whether MAMLD1 has a transactivation function for Notch targets using luciferase reporter assays [4]. Although MAMLD1 was incapable of enhancing the promoter activities of the canonical Notch target genes *Hes1* and *Hes5* with the RBP-J-binding site [22], MAMLD1 transactivated the promoter activity of the non-canonical Notch target gene *Hes3* without the RBP-J-binding site (fig. 6c) [28]. These results argue that MAMLD1 exerts its transactivation activity independent of RBP-J-binding sites. Thus, while it was predicted that MAMLD1 protein has a DNA-binding capacity, after extensive analysis, no evidence has been obtained for a positive DNA binding of MAMLD1 [4].

Furthermore, the E124X and Q197X proteins had no transactivation function, whereas the R653X protein as well as the 3 variant (P286S, Q507R, and N589S) proteins retained a nearly normal transactivating activity [4]. In addition, the transactivation function was significantly reduced in the L103P protein (an artificially constructed variant affecting the MAML motif) and normal in the ΔExon 4 [4]. These findings suggest that the E124X and Q197X proteins have no transactivation function, consistent with the inability of localizing to the nuclear bodies. However, the R653X protein, when it is artificially produced, has a normal transactivating activity, although R653X as well as E124X and Q197X have been demonstrated to undergo NMD in vivo [3, 4].

Conclusions

MAMLD1 is a causative gene for hypospadias, and possibly other forms of 46,XY DSD. It appears to play a supportive role in the testosterone production around the critical period of sex development. MAMLD1 protein localizes to the nuclear bodies and has a transactivation function for *Hes3* at least in vitro. Further studies including knockout mouse experiments will enable clarification of the *MAMLD1*-dependent molecular network involved in testosterone production.

References

1 Baskin LS, Ebbers MB: Hypospadias: anatomy, etiology, and technique. J Pediatr Surg 2007;41:463–472.
2 Achermann JC, Hughes IA: Disorders of sex development; in Kronenberg HM, Melmed S, Polonsk KS, Larsen PR (eds): Williams Textbook of Endocrinology, ed 11. Philadelphia, Saunders, 2008, pp 783–848.
3 Beleza-Meireles A, Töhönen V, Söderhäll C, Schwentner C, Radmayr C, Kockum I, Nordenskjöld A: Activating transcription factor 3: a hormone responsive gene in the etiology of hypospadias. Eur J Endocrinol 2008;158: 729–739.
4 Beleza-Meireles A, Barbaro M, Wedell A, Töhönen V, Nordenskjöld A: Studies of a cochaperone of the androgen receptor, FKBP52, as candidate for hypospadias. Reprod Biol Endocrinol 2007;5:8.
5 Beleza-Meireles A, Lundberg F, Lagerstedt K, Zhou X, Omrani D, Frisén L, Nordenskjöld A: FGFR2, FGF8, FGF10 and as candidate genes for hypospadias. Eur J Hum Genet 2007;15:405–410.
6 Watanabe M, Yoshida R, Ueoka K, Aoki K, Sasagawa I, Hasegawa T, Sueoka K, Kamatani N, Yoshimura Y, Ogata T: Haplotype analysis of the estrogen receptor 1 gene in male genital and reproductive abnormalities. Hum Reprod 2007;22:1279–1284.
7 Beleza-Meireles A, Kockum I, Lundberg F, Söderhäll C, Nordenskjöld A: Risk factors for hypospadias in the estrogen receptor 2 gene. J Clin Endocrinol Metab 2007;92: 3712–3718.
8 Fukami M, Wada Y, Miyabayashi K, Nishino I, Hasegawa T, Nordenskjöld A, Camerino G, Kretz C, Buj-Bello A, Laporte J, Yamada G, Morohashi K, Ogata T: CXorf6 is a causative gene for hypospadias. Nat Genet 2006;38: 1369–1371.
9 Fukami M, Wada Y, Okada M, Kato F, Katsumata N, Baba T, Morohashi K, Laporte J, Kitagawa M, Ogata T: Mastermind-like domain-containing 1 (MAMLD1 or CXorf6) transactivates the Hes3 promoter, augments testosterone production, and contains the SF1 target sequence. J Biol Chem 2008;283: 5525–5532.
10 Bartsch O, Kress W, Wagner A, Seemanova E: The novel contiguous gene syndrome of myotubular myopathy (MTM1), male hypogenitalism and deletion in Xq28: report of the first familial case. Cytogenet Cell Genet 1999;85:310–314.
11 Biancalana V, Caron O, Gallati S, Baas F, Kress W, Novelli G, D'Apice MR, Lagier-Tourenne C, Buj-Bello A, Romero NB, Mandel JL: Characterisation of mutations in 77 patients with X-linked myotubular myopathy, including a family with a very mild phenotype. Hum Genet 2003;112:135–142.
12 Hu LJ, Laporte J, Kress W, Kioschis P, Siebenhaar R, Poustka A, Fardeau M, Metzenberg A, Janssen EA, Thomas N, Mandel JL, Dahl N: Deletions in Xq28 in two boys with myotubular myopathy and abnormal genital development define a new contiguous gene syndrome in a 430 kb region. Hum Mol Genet 1996;5:139–143.
13 Laporte J, Guiraud-Chaumeil C, Vincent MC, Mandel JL, Tanner SM, Liechti-Gallati S, Wallgren-Pettersson C, Dahl N, Kress W, Bolhuis PA, Fardeau M, Samson F, Bertini E: Mutations in the MTM1 gene implicated in X-linked myotubular myopathy. Hum Mol Genet 1997;6:1505–1511.
14 Laporte J, Kioschis P, Hu LJ, Kretz C, Carlsson B, Poustka A, Mandel JL, Dahl N: Cloning and characterization of an alternatively spliced gene in proximal Xq28 deleted in two patients with intersexual genitalia and myotubular myopathy. Genomics 1997;41:458–462.
15 Tsai TC, Horinouchi H, Noguchi S, Minami N, Murayama K, Hayashi YK, Nonaka I, Ishino I: Characterization of MTM1 mutations in 31 Japanese families with myotubular myopathy, including a patient carrying 240 kb deletion in Xq28 without male hypogenitalism. Neuromuscul Disord 2005;15: 245–252.
16 Kuzmiak HA, Maquat LE: Applying nonsense-mediated mRNA decay research to the clinic: progress and challenges. Trends Mol Med 2006;12:306–316.
17 Morohashi K, Omura T: Ad4BP/SF-1, a transcription factor essential for the transcription of steroidogenic cytochrome P450 genes and for the establishment of the reproductive function. FASEB J 1996;10:1569–1577.
18 Ozisik G, Achermann JC, Jameson JL: The role of SF1 in adrenal and reproductive function: insight from naturally occurring mutations in humans. Mol Genet Metab 2002;76: 85–91.
19 Parker KL, Schimmer BP: Steroidogenic factor 1: a key determinant of endocrine development and function. Endocr Rev 1997;18: 361–377.
20 Lin SE, Oyama T, Nagase T, Harigaya K, Kitagawa M: Identification of new human mastermind proteins defines a family that consists of positive regulators for notch signaling. J Biol Chem 2002;277:50612–50620.
21 Wu L, Sun T, Kobayashi K, Gao P, Griffin JD: Identification of a family of mastermind-like transcriptional coactivators for mammalian notch receptors. Mol Cell Biol 2002;22:7688–7700.
22 Artavanis-Tsakonas S, Rand MD, Lake RJ: Notch signaling: cell fate control and signal integration in development. Science 1999; 284:770–776.
23 Iso T, Kedes L, Hamamori Y: HES and HERP families: multiple effectors of the Notch signaling pathway. J Cell Physiol 2003;194:237–255.
24 Nam Y, Sliz P, Song L, Aster JC, Blacklow SC: Structural basis for cooperativity in recruitment of MAML coactivators to Notch transcription complexes. Cell 2006;124:973–983.
25 Wilson JJ, Kovall RA: Crystal structure of the CSL-Notch-Mastermind ternary complex bound to DNA. Cell 2006;124:985–996.
26 Tonon G, Modi S, Wu L, Kubo A, Coxon AB, Komiya T, O'Neil K, Stover K, El-Naggar A, Griffin JD, Kirsch IR, Kaye FJ: t(11; 19)(q21; p13) translocation in mucoepidermoid carcinoma creates a novel fusion product that disrupts a Notch signaling pathway. Nat Genet 2003;33:208–213.
27 Androutsellis-Theotokis A, Leker RR, Soldner F, Hoeppner DJ, Ravin R, Poser SW, Rueger MA, Bae SK, Kittappa R, McKay RD: Notch signalling regulates stem cell numbers in vitro and in vivo. Nature 2006;442: 823–826.
28 Nishimura M, Isaka F, Ishibashi M, Tomita K, Tsuda H, Nakanishi S, Kageyama R: Structure, chromosomal locus, and promoter of mouse Hes2 gene, a homologue of Drosophila hairy and Enhancer of split. Genomics 1998;49:69–75.

Endocrine Journal 2010, 57 (2), 171-174

Diabetes Mellitus in a Japanese Girl with HDR Syndrome and *GATA3* Mutation

KOJI MUROYA[1),2)], TAKAHIRO MOCHIZUKI[3)], MAKI FUKAMI[1)], MANAMI ISO[1)], KEINOSUKE FUJITA[3)], MITSUO ITAKURA[4)] AND TSUTOMU OGATA[1)]

[1)] *Department of Endocrinology and Metabolism, National Research Institute for Child Health and Development, Tokyo, Japan*
[2)] *Department of Endocrinology and Metabolism, Kanagawa Children's Medical Center, Yokohama, Japan*
[3)] *Department of Pediatrics, Children's Medical Center, Osaka City General Hospital, Osaka, Japan*
[4)] *Institute for Genome Research, Tokushima University, Tokushima, Japan*

Abstract. We report on a Japanese girl with HDR (*h*ypoparathyroidism, sensorineural *d*eafness, and *r*enal dysplasia) syndrome who developed diabetes mellitus (DM) at three years of age (blood glucose 713 mg/dL, HbA_{1c} 8.0%) in the absence of anti-glutamic acid decarboxylase autoantibodies. Mutation analysis revealed a *de novo* heterozygous two base pair deletion at exon 6 of the *GATA3* gene (c.1200_1201delCA; p.H400fsX506). *GATA3* expression was identified by PCR amplification for human pancreas cDNA, and mouse *Gata3* was weekly but unequivocally expressed in pancreatic β cells. The results, in conjunction with the previous findings indicating the critical role of *GATA3* in lymphocyte function, suggest that *GATA3* haploinsufficiency may affect the function of β cells and/or lymphocytes, leading to the development of DM in relatively exceptional patients with high susceptibility to DM.

Key words: Diabetes mellitus, Expression, *GATA3*, HDR syndrome

HDR (*h*ypoparathyroidism, sensorineural *d*eafness, and *r*enal dysplasia) syndrome is an autosomal dominant disorder first reported by Bilous *et al.* [1]. This condition is primarily caused by haploinsufficiency of *GATA3* on chromosome 10p15, although a *GATA3* mutation has not been identified in several patients with HDR syndrome-compatible clinical features [2, 3]. *GATA3* consists of six exons, and encodes a transcription factor with two transactivation domains and two zinc finger domains [2]. *GATA3* is expressed in the developing parathyroid glands, inner ears, and kidneys, together with thymus and central nervous system [4, 5]. While several non-triad features such as pyloric stenosis, ventricular septal defect, polycystic ovary, abnormal Müllerian duct structures, and hemimegalencephaly have been described in several patients with *GATA3* mutations [3, 6–8], there is no report documenting diabetes mellitus (DM) in this condition.

Here, we report a patient with DM and a *GATA3* mutation, and discuss a potential relationship between DM and a *GATA3* mutation.

Received Oct. 26, 2009; Accepted Nov. 19, 2009 as K09E-313
Released online in J-STAGE as advance publication Dec. 1, 2009

Correspondence to: Dr. Tsutomu OGATA, Department of Endocrinology and Metabolism, National Research Institute for Child Health and Development, 2-10-1 Ohkura, Setagaya, Tokyo 157-8535, Japan. E-mail: tomogata@nch.go.jp

Case Report

This Japanese girl was born at 37 weeks of gestation after an uncomplicated pregnancy and delivery. At birth, her length was 43.0 cm (–2.4 SD) and her weight 1.74 kg (–3.1 SD). The non-consanguineous parents and the younger brother were clinically normal.

At 3 months of age, she was admitted to Osaka City Medical Center because of frequent vomiting and irritability. Routine laboratory tests revealed hypocalcemia (7.8 mg/dL) (age- and sex-matched Japanese reference value, 9.8–11.6 mg/dL) and hyperphosphatemia (8.3 mg/dL) (5.1–7.1 mg/dL), and subsequent biochemical studies showed parathyroid hormone (PTH) deficiency (intact PTH, below 5 pg/mL) (10–50 pg/mL). Thus, 1α-(OH) vitamin D therapy was started, successfully normalizing serum calcium and phosphate values. At 12 months of age, since she

responded poorly to sounds, auditory brainstem response was performed, indicating severe sensorineural deafness with hearing levels being 80 dB for the right ear and 100 dB for the left ear (normal range, below 25 dB). Thus, hearing aids were utilized in her daily life.

At 3 years of age, she showed polydipsia, polyuria, and weight loss, and was diagnosed as having DM because of elevated blood glucose (713 mg/dL) (70–110 mg/dL) and HbA_{1c} (8.0%) (4.3–5.8%). Serum insulin was 8.0 μU/mL (1.7–10.4μU/mL) and C-peptide 1.1 ng/mL (0.6–1.8 ng/mL). She was immediately placed on insulin therapy (~0.7 U/kg/day). Urine C-peptide gradually decreased and became undetectable at eight years of age; at that time, she required insulin therapy of 1.08 U/kg/day. Anti-glutamic acid decarboxylase autoantibodies (anti-GAD Abs) were negative throughout the clinical course. At nine years of age, she was found to have elevated blood urea nitrogen (61.3 mg/dL) (7.5–19.3 mg/dL) and creatinine (2.0 mg/dL) (0.4–0.8 mg/dL) at the time of periodical follow-up examinations for DM. Thus, renal echography and scntigraphy were performed, showing right renal aplasia and left renal hypoplasia. Other abdominal visceral organs including the pancreas exhibited apparently normal structures on the ultrasound examinations. Chromosome analysis revealed a 46,XX karyotype in all the 50 lymphocytes examined. On the basis of the above findings, she was diagnosed as having HDR syndrome and DM. At present, she is 12 years old, and shows short stature (–4.5 SD) and some pubertal development (breast, Tanner stage 2). Current insulin dosage is 1.17 U/kg/day, and her DM has been well controlled with HbA1c value being maintained around 6.0%.

Methods

Mutation analysis of GATA3

This study was approved by the Institutional Review Board Committee at National Center for Child Health and Development. After obtaining informed consent, leukocyte genomic DNA samples of the patient and the parents were PCR-amplified for the coding exons 2–6 and their splice sites, and the PCR products were subjected to direct sequencing from both directions on a CEQ 8000 autosequencer (Beckman Coulter, Fullerton, CA). The primer sequences and the PCR conditions were as described previously [2, 3]. To confirm a heterozygous mutation, the corresponding PCR products were subcloned with a TOPO TA Cloning Kit (Invitrogen, Carlsbad, CA), and normal and mutant alleles were sequenced separately.

PCR amplification of human pancreas cDNA

Human pancreas cDNA was purchased from Clontech (Mountain View, CA), as well as fetal kidney cDNA utilized as a positive control. PCR amplification was performed with 0.5 ng of cDNA samples, using the forward primer for exon 5 (5'–GAATGCCA-ATGGGGACCCTGT–3') and the reverse primer for exon 6 (5'–TTCATGCCTTACAGCTACCCAGA–3').

In situ hybridization (ISH) analysis for the mouse pancreas

Fifteen-week-old female BDF1 mice (Clea Japan, Tokyo) were anesthetized with sodium pentobarbital and fixed by cardiac perfusion with Mildform10N (Wako Pure Chemical Industries, Osaka). Pancreatic tissues were dissected and fixed with the same fixative for 48 hours at room temperature. The tissues were embedded in paraffin, and serial tissue sections were prepared at 5 μm thickness. ISH analysis was performed with BlueMap Kit and Discovery automatic staining modules (Ventana Medical Systems, Tucson, AZ) according to manufacturer's instructions. cDNAs of mouse *Ins-1* (an insulin-like peptide orthologous to human insulin) (nt 653–1117, GenBank accession no. X04725) and *Gata3* (nt 1566–2002, GenBank accession no. NM_008091) were amplified by reverse transcription PCR and subcloned into pCR4Blunt-TOPO (Invitrogen). Sense and antisense digoxigenin-labeled RNA probes were synthesized using T7 or T3 RNA polymerase in the presence of digoxigenin-labeled dUTP following the manufacturer's protocol (Roche Molecular Biochemicals, Indianapolis, IN).

Results

Mutation analysis of GATA3

This patient had a heterozygous two base pair deletion at exon 6 (c.1200_1201delCA) of *GATA3* that is predicted to cause a frameshift at the 400th codon for the histidine and resultant termination at the 506th codon (p.H400fsX506) (Fig. 1). This mutation was absent from the parents.

PCR amplification of human pancreas cDNA

PCR products of 690 bp long were identified in fe-

tal kidney after 25 cycles and in pancreas after 40 cycles (Fig. 2A). This indicated relatively weak *GATA3* expression in the pancreas.

ISH analysis for the mouse pancreas

Anti-sense probes for *Gata3* detected weak but definitive signals in cells with strong *Ins-1* expression (Fig. 2B). This showed specific *Gata3* expression in the mouse pancreatic β cells.

Discussion

This patient had the triad of the HDR syndrome and a heterozygous mutation of *GATA3*. This is consistent with the previous data indicating that *GATA3* mutations are usually identified in patients with two or three of the HDR triad features [9, 10].

The salient feature of this patient is the development of DM. This may be co-incidental, because DM has not been identified in patients with *GATA3* mutations. However, human *GATA3* was identified in the human pancreas cDNA sample, and mouse *Gata3* was weekly but unequivocally expressed in pancreatic β cells. In addition, *GATA3* is known to play an important role in lymphocyte development and function [11, 12]. Thus, *GATA3* haploinsufficiency may affect the function of β cells and/or lymphocytes, leading to the development of DM in relatively exceptional patients with high susceptibility to DM because of other genetic and environmental factors. In this regard, the absence of anti-GAD Abs may argue for possible β cell, rather than lymphocyte, dysfunction [13].

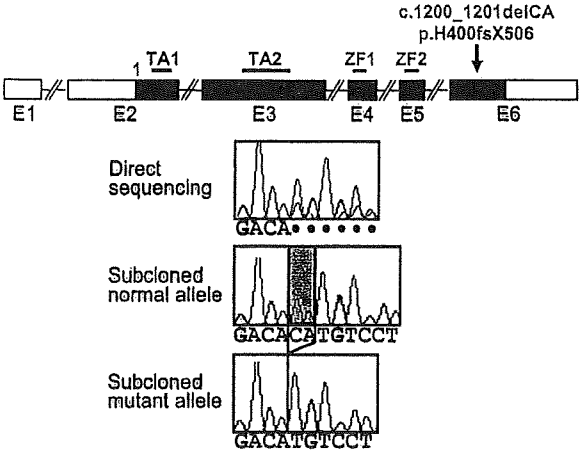

Fig. 1. Mutation analysis of *GATA3*.
Upper diagram: The genomic structure of *GATA3*. The black and white boxes denote the coding and the untranslated regions, respectively. TA1 and TA2 denote two transactivation domains, and ZF1 and ZF2 represent two zinc finger domains.
Lower diagram: The electrochromatograms delineate the c.1200_1201delCA (p.H400fsX506) mutation at exon 6. This mutation has been indicated by the direct sequencing, and confirmed by the subsequently performed sequencing of the subcloned normal and mutant alleles.

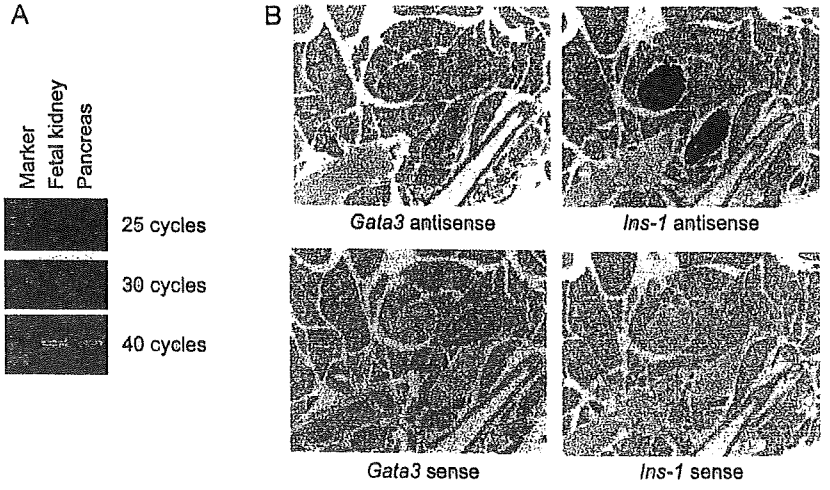

Fig. 2. Expression analyses of *GATA3/Gata3*.
A. PCR-amplification using human cDNA samples. *GATA3* expression is identified after 25 cycles in the fetal kidney, and after 40 cycles in the pancreas.
B. ISH analysis using the mouse pancreas. The antisense probe for *Gata3* detects weak but positive signals in the cells with strong expression of *Ins-1* (β cells). No signals have been identified by the sense probes.

The frameshift mutation resided on the last coding exon 6. Since the position of the mutation satisfies the condition for the escape from nonsense mediated mRNA decay [14], it is possible that an aberrant GATA3 protein is produced, leading to the development of DM due to a dominant negative effect. However, this possibility is unlikely, because previously reported patients with nonsense or frameshift mutations on exon 6 are free from DM [3, 10].

In summary, we observed a patient with a *GATA3* mutation and DM. Further studies will clarify whether *GATA3* mutations can be a risk factor for the development of DM.

Acknowledgements

This work was supported in part by grants for Child Health and Development and for Research on Children and Families from the Ministry of Health, Labor, and Welfare.

References

1. Bilous RW, Murty G, Parkinson DB, Thakker RV, Coulthard MG, Burn J, Mathias D, Kendall-Taylor P (1992) Autosomal dominant familial hypoparathyroidism, sensorineural deafness, and renal dysplasia. *N Engl J Med* 327: 1069–1074.
2. Van Esch H, Groenen P, Nesbit MA, Schuffenhauer S, Lichtner P, Vanderlinden G, Harding B, Beetz R, Bilous RW, Holdaway I, Shaw NJ, Fryns JP, Van de Ven W, Thakker RV, Devriendt K (2000) GATA3 haplo-insufficiency causes human HDR syndrome. *Nature* 406: 419–422.
3. Muroya K, Hasegawa T, Ito Y, Nagai T, Isotani H, Iwata Y, Yamamoto K, Fujimoto S, Seishu S, Fukushima Y, Hasegawa Y, Ogata T (2001) GATA3 abnormalities and the phenotypic spectrum of HDR syndrome. *J Med Genet* 38: 374–380.
4. Labastie MC, Catala M, Gregoire JM, Peault B (1995) The GATA3 gene is expressed during human kidney embryogenesis. *Kidney Int* 47: 1597–1603.
5. Debacker C, Catala M, Labastie MC (1999) Embryonic expression of the human GATA3 gene. *Mech Dev* 85: 183–187.
6. Zahirieh A, Nesbit MA, Ali A, Wang K, He N, Stangou M, Bamichas G, Sombolos K, Thakker RV, Pei Y (2005) Functional analysis of a novel GATA3 mutation in a family with the hypoparathyroidism, deafness, and renal dysplasia syndrome. *J Clin Endocrinol Metab* 90: 2445–2450.
7. Hernández AM, Villamar M, Roselló L, Moreno-Pelayo MA, Moreno F, Del Castillo I (2007) Novel mutation in the gene encoding the GATA3 transcription factor in a Spanish familial case of hypoparathyroidism, deafness, and renal dysplasia (HDR) syndrome with female genital tract malformations. *Am J Med Genet A* 143: 757–762.
8. Adachi M, Tachibana K, Asakura Y, Tsuchiya T (2006) A novel mutation in the GATA3 gene in a family with HDR syndrome (hypoparathyroidism, sensorineural deafness and renal anomaly syndrome). *J Pediatr Endocrinol Metab* 19: 87–92.
9. Nesbit MA, Bowl MR, Harding B, Ali A, Ayala A, Crowe C, Dobbie A, Hampson G, Holdaway I, Levine MA, McWilliams R, Rigden S, Sampson J, Williams AJ, Thakker RV (2004) Characterization of GATA3 mutations in the hypoparathyroidism, deafness, and renal dysplasia (HDR) syndrome. *J Biol Chem* 279: 22624–22634.
10. Ali A, Christie PT, Grigorieva IV, Harding B, Van Esch H, Ahmed SF, Bitner-Glindzicz M, Blind E, Bloch C, Christin P, Clayton P, Gecz J, Gilbert-Dussardier B, Guillen-Navarro E, Hackett A, Halac I, Hendy GN, Lalloo F, Mache CJ, Mughal Z, Ong AC, Rinat C, Shaw N, Smithson SF, Tolmie J, Weill J, Nesbit MA, Thakker RV (2007) Functional characterization of GATA3 mutations causing the hypoparathyroidism-deafness-renal (HDR) dysplasia syndrome: insight into mechanisms of DNA binding by the GATA3 transcription factor. *Hum Mol Genet* 16: 265–275.
11. Labastie MC, Bories D, Chabret C, Grégoire JM, Chrétien S, Roméo PH (1994) Structure and expression of the human GATA3 gene. *Genomics* 21: 1–6.
12. Hendriks RW, Nawijn MC, Engel JD, van Doorninck H, Grosveld F, Karis A (1999) Expression of the transcription factor GATA-3 is required for the development of the earliest T cell progenitors and correlates with stages of cellular proliferation in the thymus. *Eur J Immunol* 29: 1912–1918.
13. Eisenabrth GS, Polonsky KS, Buse JB (2008) Type 1 diabetes mellitus. In: Kronenberg HM, Melmed S, Polonsky KS, Larsen PR (eds). Williams textbook of endocrinology, 11th ed. W.B. Saunders, Philadelphia, pp 1391–1416.
14. Kuzmiak HA, Maquat LE (2006) Applying nonsense-mediated mRNA decay research to the clinic: progress and challenges. *Trends Mol Med* 12: 306–316.

Novel Insights from Clinical Practice

HORMONE RESEARCH

Horm Res 313
DOI: 10.1159/000XXXXXX

Received: September 7, 2009
Accepted: November 11, 2009
Published online: ■■■

Hypothalamic Dysfunction in a Female with Isolated Hypogonadotropic Hypogonadism and Compound Heterozygous *TACR3* Mutations and Clinical Manifestation in Her Heterozygous Mother

Maki Fukami[a] Tetsuo Maruyama[b] Sumito Dateki[a] Naoko Sato[a]
Yasunori Yoshimura[b] Tsutomu Ogata[a]

[a]Department of Endocrinology and Metabolism, National Research Institute for Child Health and Development, and
[b]Department of Obstetrics and Gynecology, Keio University School of Medicine, Tokyo, Japan

Established Facts

- *TAC3* and *TACR3* have recently been shown to be causative genes for an autosomal recessive form of isolated hypogonadotropic hypogonadism (IHH).

Novel Insights

- Hypothalamic dysfunction may be the primary cause for IHH in patients with biallelic *TACR3* mutations.
- Clinical phenotype may be exhibited by females with heterozygous *TACR3* mutations.
- *TAC3* and *TACR3* mutations remain rare in patients with IHH.

Key Words
Heterozygous manifestation · Hypogonadotropic hypogonadism · Hypothalamus · *TACR3* mutation

Abstract
Background/Aims: *TAC3* and *TACR3* have recently been shown to be causative genes for an autosomal recessive form of isolated hypogonadotropic hypogonadism (IHH). Here, we report a Japanese female with IHH and compound heterozygous *TACR3* mutations and her heterozygous parents, and discuss the primary lesion for IHH and clinical findings. ***Case Report:*** This female was identified through mutation analysis of *TAC3* and *TACR3* in 57 patients with IHH. At 24 years of age, an initial standard GnRH test showed poor gonadotropin response (LH <0.2–0.6 IU/l), whereas the second GnRH test performed after GnRH priming (100 μg i.m. for 5

This work was supported by grants from the Ministry of Health, Labor, and Welfare, and the Ministry of Education, Culture, Sports, Science, and Technology.

KARGER
Fax +41 61 306 12 34
E-Mail karger@karger.ch
www.karger.com

0301–0163/10/0000–0000$26.00/0

Accessible online at:
www.karger.com/hre

Tsutomu Ogata
Department of Endocrinology and Metabolism
National Research Institute for Child Health and Development
2-10-1 Ohkura, Setagaya, Tokyo 157-8535 (Japan)
Tel. +81 3 5494 7025, Fax +81 3 5494 7026, E-Mail tomogata@nch.go.jp

consecutive days) revealed ameliorated gonadotropin responses (LH 0.3–6.4 IU/l; FSH 2.2–9.6 IU/l). The mother exhibited several features suggestive of mild IHH, whereas the father showed an apparently normal phenotype. ***Results:*** She had a paternally derived nonsense mutation at exon 1 (Y145X) and a maternally inherited single nucleotide (G) deletion from the conserved 'GT' splice donor site of intron 1 (IVS1+1delG). ***Conclusions:*** The results suggest hypothalamic dysfunction as the primary cause for IHH in patients with biallelic *TACR3* mutations and clinical manifestation in heterozygous females, together with the rarity of *TAC3* and *TACR3* mutations in patients with IHH.

Introduction

Isolated hypogonadotropic hypogonadism (IHH) is a genetically heterogeneous condition that lacks other pituitary hormone deficiency [1]. Recently, Topaloglu et al. [2] and Guran et al. [3] have reported homozygous *TAC3* or *TACR3* missense mutations in 11 patients with IHH from 5 Turkish or Kurdish families. TAC3 belongs to an evolutionally conserved neuropeptide family, and TACR3 belongs to a G-protein-coupled receptor family [4]. Topaloglu et al. [2] and Guran et al. [3] also performed functional studies using an intracellular calcium flux system, successfully revealing markedly attenuated activities of the TAC3 and TACR3 mutant proteins. These data provide the first evidence of genetic defects in TAC3/TACR3 signaling being involved in an autosomal recessive form of IHH.

However, there is no other report of *TAC3* or *TACR3* mutations, and further studies are necessary to define the underlying factor(s) for IHH and clinical findings in *TAC3* or *TACR3* mutations. Here, we report a female with IHH and *TACR3* mutations, and discuss the primary cause for IHH and the clinical phenotypes of the patient and her heterozygous parents.

Methods

Mutation Analysis

This study was approved by the Institutional Review Board Committees at the National Center for Child Health and Development and Keio University School of Medicine. After obtaining written informed consent, leukocyte genomic DNA samples from 57 Japanese cases with IHH (38 with 46,XY and 19 with 46,XX) were PCR-amplified with the previously reported primers [2], and subjected to direct sequencing on a CEQ 8000 autosequencer (Beckman Coulter, Fullerton, Calif., USA). To confirm a heterozygous mutation, the corresponding PCR products were subcloned with a TOPO TA Cloning Kit (Invitrogen, Carlsbad, Calif., USA), and the two alleles were sequenced separately.

Prediction of Aberrant Splicing and Nonsense-Mediated mRNA Decay

We utilized the splice site prediction program at the Berkeley Drosophila Genome Project (http://www.fruitfly.org/seq_tools/splice.html) to predict aberrant splicing. On the basis of the previous report [5], we also analyzed whether identified mutations could be subject to nonsense-mediated mRNA decay (NMD) that functions as an mRNA surveillance mechanism to prevent the formation of aberrant proteins.

PCR-Based cDNA Screening for TACR3

Human cDNA samples from control subjects were prepared by RT-PCR or purchased from Clontech (Palo Alto, Calif., USA). PCR amplification was performed for *TACR3* with primers for exon 1 (5′-TTGTGAACCTGGCTTTCTCC-3′) and exon 3 (5′-GGATTTCTCCTCCCCAGAGA-3′), as well as for *GAPDH* utilized as an internal control with primers for the boundary of exons 2/3 (5′-TCGGAGTCAACGGATTTGGTCG-3′) and the boundary of exons 4/5 (5′-TTGGAGGGATCTCGCTCCTG-3′).

Results

Mutation Analysis

Mutation analysis identified two heterozygous mutations of *TACR3* in a female patient, i.e. a nonsense mutation at exon 1 (Y145X) and a single nucleotide (G) deletion from the conserved 'GT' splice donor site of intron 1 (IVS1+1delG; fig. 1A, B). The father was heterozygous for Y145X, and the mother was heterozygous for IVS1+1delG. No demonstrable mutation was detected for *TAC3* in this patient and for *TAC3* and *TACR3* in the remaining 56 cases.

Prediction of Aberrant Splicing and NMD

The IVS1+1delG mutation was predicted to add a 1,153-bp intronic sequence to exon 1 and to cause aberrant splice formation between the added sequence and the normal splice acceptor site of exon 2 (fig. 1C). Furthermore, because of the presence of a stop codon on the added intronic sequence, the IVS1+1delG mutation was predicted to cause a premature termination at the 210th codon. Thus, both IVS1+1delG and Y145X satisfied the conditions for the occurrence of NMD.

PCR-Based cDNA Screening for TACR3

TACR3 expression was clearly identified in the hypothalamus and the pituitary as well as in the whole brain, the ovary, the placenta, and the fetal kidney, but not detected in the testis and leukocytes (fig. 2).

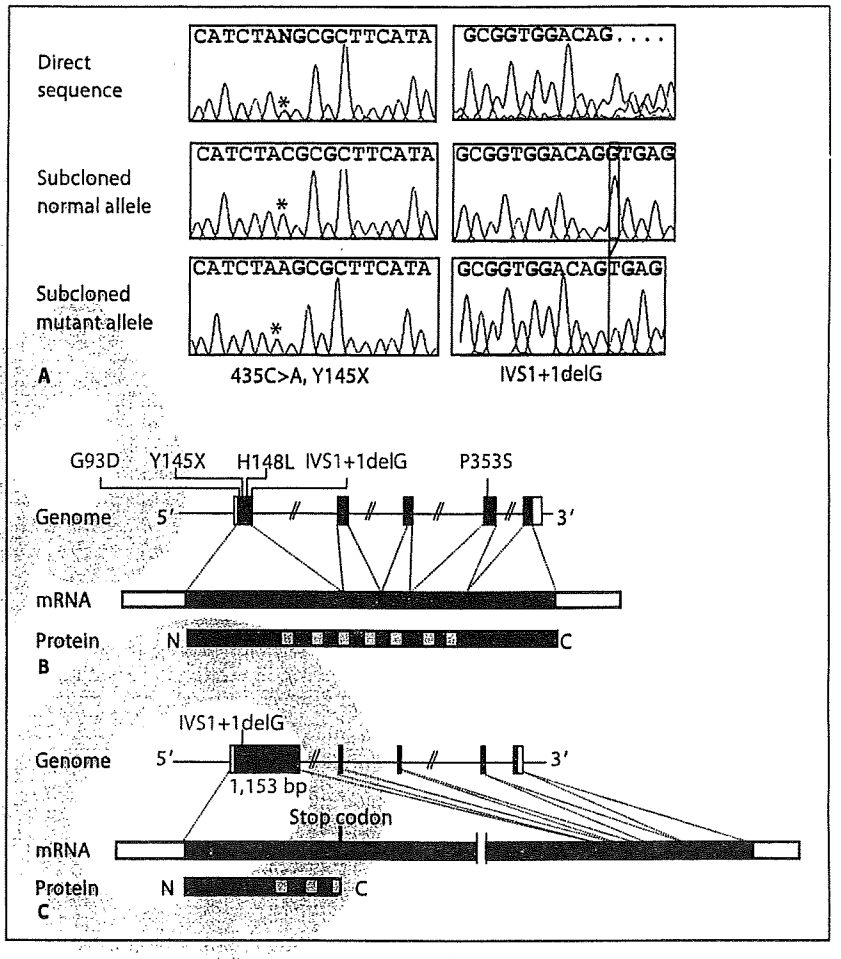

Fig. 1. *TACR3* mutations of the female Japanese patient. **A** Electrochromatograms showing 435C>A (Y145X; indicated by asterisks) and IVS1+1delG (highlighted by red lines). The mutation was indicated by direct sequencing, and confirmed by the subsequently performed sequencing of the subcloned normal and mutant alleles. **B** Schematic presentation of the positions of the mutations. The gray and white boxes on genomic DNA (Genome) and mRNA indicate the coding regions and the untranslated regions on exons 1–5. TACR3 protein (Protein) harbors 7 transmembrane domains (yellow boxes). The mutations identified in the Japanese patient are shown in red, and those reported by Topaloglu et al. [2] and Guran et al. [3] are shown in blue. **C** Predicted consequences of the IVS1+1delG mutation. In silico analysis indicates that IVS1+1delG causes addition of 1,153-bp intronic sequences (green box) to exon 1 and an aberrant splice formation between the added sequence and the normal splice acceptor site of exon 2. The transcribed intronic sequence (green box) harbors a stop codon on its very proximal 5′ region.

Case Report

This Japanese female patient was born as the sole child to nonconsanguineous parents at 42 weeks of gestation after an uncomplicated pregnancy and delivery. Her postnatal growth and development were normal until pubertal age. At 19 years of age, she was seen at a local clinic because of primary amenorrhea. She exhibited poor pubertal development (breast, Tanner stage 1; pubic hair, stage 2), with low basal gonadotropin and estradiol values (table 1). Thus, she received cyclic estrogen and progesterone therapy, and showed periodic withdrawal bleeding. She showed markedly high educational achievement at a university.

At 24 years of age, she was referred to us for further investigations. She measured 163 cm (+0.7 SD) and weighed 48.5 kg (–0.6 SD). Her breast development was at Tanner stage 3–4, and her pubic hair at stage 4. Magnetic resonance imaging delineated normal pituitary structure. Basal blood hormone values measured at 4 weeks after discontinuation of the hormone replacement therapy were consistent with IHH (table 1). Furthermore, while an initial standard GnRH test showed a poor gonadotropin response, the second-time GnRH test performed after GnRH priming (100 μg i.m. for 5 consecutive days) revealed obviously ameliorated gonadotropin responses (table 1).

The 58-year-old mother had menarche at 14.6 years of age (the menarchial age of Japanese females is 9.75–14.75 years). Subsequently, she had regular but long (~45 days) menstrual cycles with occasionally slight intermenstrual bleeding. She had no signs of androgen excess such as hirsutism. She married at 25 years of age, and failed to conceive for 3 years despite an ordinary conjugal life. Basal body temperature records indicated frequent, though not invariable, occurrence of monophasic cycles. Thus, she was treated with chlomiphene citrate by a local medical doctor, and became pregnant at the second cycle of this therapy. Polycystic ovary was excluded by repeatedly performed ultrasound studies during pregnancy. Her menses became irregular from ~45 years of age and ceased at 56 years of age (the menopausal age of Japanese females is 45–56 years). She was otherwise healthy with normal stature (150 cm, –0.5 SD for her age) and intelligence. The 59-year-old father was clinically normal with normal stature (168 cm, +0.9 SD for his age) and intelligence. Allegedly, he had an age-appropriate pubertal development and started shaving at 16 years of age.